

Article

The Search for New Antibacterial Agents among 1,2,3-Triazole Functionalized Ciprofloxacin and Norfloxacin Hybrids: Synthesis, Docking Studies, and Biological Activity Evaluation

Halyna Hryhoriv ¹, Illia Mariutsa ² , Sergiy M. Kovalenko ³ , Victoriya Georgiyants ¹ , Lina Perekhoda ⁴, Nataliia Filimonova ⁵ , Olga Geyderikh ⁵ and Lyudmila Sidorenko ^{1,*} 

¹ Pharmaceutical Chemistry Department, National University of Pharmacy, 61153 Kharkiv, Ukraine; galkagrigoriv@gmail.com (H.H.); vgeor@ukr.net (V.G.)

² Organic Chemistry Department, National University of Pharmacy, 61153 Kharkiv, Ukraine; mariutsaillia@gmail.com

³ Organic Chemistry Department, V. N. Karazin Kharkiv National University, 61022 Kharkiv, Ukraine; kovalenko.sergiy.m@gmail.com

⁴ Medicinal Chemistry Department, National University of Pharmacy, 61153 Kharkiv, Ukraine; linaperekhoda@ukr.net

⁵ Department of Microbiology, National University of Pharmacy, Virology and Immunology, 61153 Kharkiv, Ukraine; natafilimanova@gmail.com (N.F.); ogejderih@gmail.com (O.G.)

* Correspondence: slv.ludmila16@gmail.com



Citation: Hryhoriv, H.; Mariutsa, I.; Kovalenko, S.M.; Georgiyants, V.; Perekhoda, L.; Filimonova, N.; Geyderikh, O.; Sidorenko, L. The Search for New Antibacterial Agents among 1,2,3-Triazole Functionalized Ciprofloxacin and Norfloxacin Hybrids: Synthesis, Docking Studies, and Biological Activity Evaluation. *Sci. Pharm.* **2022**, *90*, 2. <https://doi.org/10.3390/scipharm90010002>

Academic Editor: Osvaldo Andrade Santos-Filho

Received: 19 November 2021

Accepted: 16 December 2021

Published: 22 December 2021

Publisher's Note: MDPI stays neutral with regard to jurisdictional claims in published maps and institutional affiliations.



Copyright: © 2021 by the authors. Licensee MDPI, Basel, Switzerland. This article is an open access article distributed under the terms and conditions of the Creative Commons Attribution (CC BY) license (<https://creativecommons.org/licenses/by/4.0/>).

Abstract: Among all modern antibiotics, fluoroquinolones are well known for their broad spectrums of activity and efficiency toward microorganisms and viruses. However, antibiotic resistance is still a problem, which has encouraged medicinal chemists to modify the initial structures in order to combat resistant strains. Our current work is aimed at synthesizing novel hybrid derivatives of ciprofloxacin and norfloxacin and applying docking studies and biological activity evaluations in order to find active promising molecules. We succeeded in the development of a synthetic method towards 1,2,3-triazole-substituted ciprofloxacin and norfloxacin derivatives. The structure and purity of the obtained compounds were confirmed by ¹H NMR, ¹³C NMR, ¹⁹F NMR, LC/MS, UV-, IR- spectroscopy. Docking studies, together with in vitro research against *Staphylococcus aureus* ATCC 25923, *Escherichia coli* ATCC 25922, *Bacillus subtilis* ATCC 6633, *Pseudomonas aeruginosa* ATCC 27853, *Candida albicans* NCTC 885-653 revealed compounds in which activity exceeded the initial molecules.

Keywords: fluoroquinolones; ciprofloxacin; norfloxacin; synthesis; antibiotic resistance; molecular docking; antibacterial activity

1. Introduction

As the COVID-19 pandemic progresses, the task of finding a perfect form of therapy for this disease is becoming increasingly challenging. Clinicians need to make daily decisions and prescribe existing medicines, even when the data about their activities, in this case, are absent. Throughout the world, medicinal chemists are searching for effective remedies among existing antibiotics and antivirals.

Investigations have been made to analyze antibiotic prescribing practices for patients with COVID-19. According to the authors of [1], a combination of beta-lactams and macrolides or fluoroquinolones are reported in most cases.

Among these groups of antibiotics, fluoroquinolones are known as broad-spectrum synthetic antimicrobials. Their development started in the early 1960s, with the nalidixic acid synthesis; since then, four generations of highly efficient fluoroquinolones have been created [2] (Figure 1).

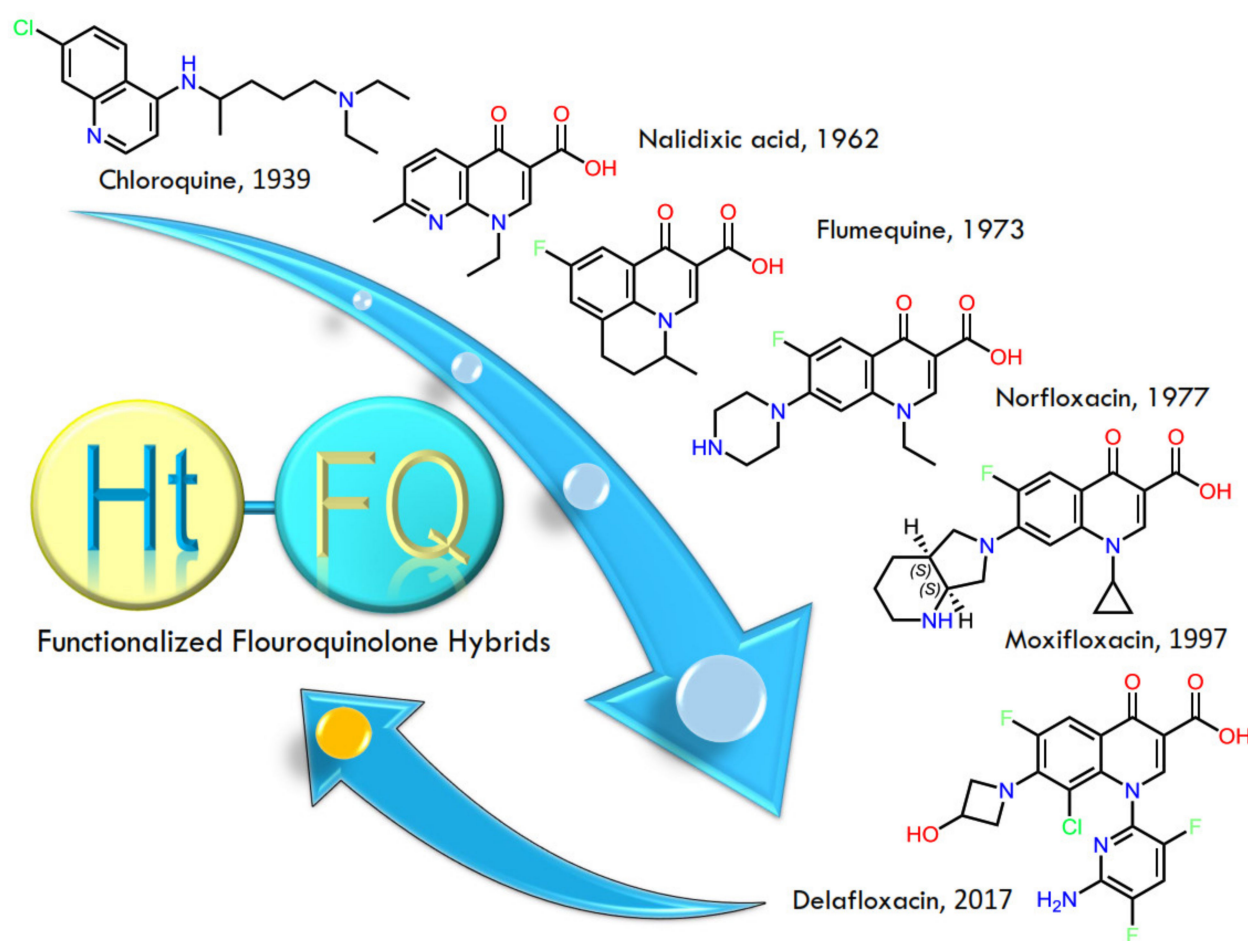


Figure 1. Evolutionary trends of quinolone APIs.

General fluoroquinolone structures contain a bicyclic system that is substituted at the N-1 position, has a carboxyl group at position 3, an oxo group at position 4, a fluorine atom at the 6-position, and a substituent (often nitrogen-based heterocyclic moiety) at C-7 [3]. Different structural modifications through a wide range of synthetic approaches are possible in each of the above-mentioned positions, mainly aimed at changing pharmacodynamics and pharmacokinetics of the initial molecules [4–6]. Therefore, such a vast family of synthetic antibiotics have evolved because of the attractiveness of fluoroquinolones from the viewpoint of chemists.

Moreover, novel molecules of fluoroquinolones were created in order to cope with the problem of resistance to antibiotics [7,8], and to increase the effectiveness along with decreasing the side effects. In this way, the concept of a hybrid design of medicines, which utilizes several pharmacophores and unites them in one molecule, appears to be of high interest.

Recently, the authors of [9] reported that the fluoroquinolones—levofloxacin and moxifloxacin—are the most commonly used antimicrobial agents for the treatment of chronic obstructive pulmonary disease and community-acquired pneumonia. Noteworthy, they not only reveal wide antimicrobial activity, but also possess antiviral action against vaccinia virus, papovavirus, CMV, VZV, HSV-1, HSV-2, HCV, and HIV [10].

It is no wonder that, through the COVID-19 pandemic, scientists have turned their attention towards fluoroquinolones as possible medicines for treatment, and there are already some promising results. The authors of [11] conducted an *in silico* molecular docking study, and demonstrated for the first time the ability of ciprofloxacin and moxifloxacin to interact with the COVID-19 main protease. Another group [12] described low antiviral activity

potency of four fluoroquinolones (enoxacin, ciprofloxacin, levofloxacin, and moxifloxacin) against SARS-CoV-2 and MERS-CoV.

According to the above-mentioned information, we chose fluoroquinolones, namely norfloxacin and ciprofloxacin, as the objects for investigation and creation of new hybrid drugs.

We should note that norfloxacin and ciprofloxacin have become popular starting molecules, as many recent studies used them to synthesize new derivatives. They represent the second generation of fluoroquinolones, and the first ones with the fluorine atom at C-6. However, while they were widely used in clinical practices, the problem of antibiotic resistance has erupted, and led to the creation of third- and fourth-generation of fluoroquinolones.

However, norfloxacin and ciprofloxacin are still utilized in medicinal chemistry, and modifications of their structures often provide inspiring results. Research for new antibacterials mainly focuses on the C-7 position. First, substituents here are important for the spectrum and potency of fluoroquinolone action. Moreover, chemical modifications at C-7 possess influence on pharmacokinetic properties and cell permeability of molecules. Additionally, paper [13] shows that the C-7 substituent has a great impact on the interaction with the target enzyme DNA gyrase.

According to the literature data, nitrogen in piperazine ring can be modified with such heterocyclic moieties as phenylthiazole [13], thiazolidine [14], quinazoline [15], thiadiazole [16,17], pyrimidine [18,19], dithienylethene [20], and 1,2,4-triazole [21]. Azole functionalized hybrids revealed promising levels of antibacterial activity [22], which led us to assume the effectiveness of 1,2,3-triazole moiety utilization for hybrid modification of fluoroquinolones.

It is also worth mentioning that our previous experience in quinolones chemistry [23–25] gave a powerful background for the planning stage of this research.

Therefore, the main purpose of our scientific team was to synthesize novel 1,2,3-triazole substituted derivatives of fluoroquinolones norfloxacin and ciprofloxacin, and to use docking and in vitro studies to find new hybrid molecules with antimicrobial activity.

2. Materials and Methods

2.1. Chemicals and Apparatus

The starting fluoroquinolones were commercially available; they, as well as the solvents, were purchased from Sigma Aldrich, St. Louis, MO 68178, The United States, and were used without further purification.

All NMR spectra were recorded on a Varian MR-400 spectrometer with standard pulse sequences operating at 400 MHz for ^1H NMR, 101 MHz for ^{13}C NMR, and 376 MHz for ^{19}F NMR. For all NMR spectra, DMSO- d_6 was used as a solvent. Chemical shift values are referenced to residual protons (δ 2.49 ppm) and carbons (δ 39.6 ppm) of the solvent as an internal standard. Elemental analysis was performed on a EuroEA-3000 CHNS-O analyzer. Melting points were determined with a Buchi B-520 melting point apparatus. LC/MS spectra were recorded on an ELSD Alltech 3300 liquid chromatograph equipped with a UV detector (λ_{max} 254 nm), API-150EX mass-spectrometer, and using a Zorbax SB-C18 column, Phenomenex (100 \times 4 mm) Rapid Resolution HT cartridge 4.6 \times 30 mm, 1.8-Micron. Elution started with 0.1 M solution of HCOOH in water and ended with 0.1 M solution of HCOOH in acetonitrile, using a linear gradient at a flow rate of 0.15 mL/min and an analysis cycle time of 25 min. IR spectra in KBr pellets were recorded on a Perkin-Elmer 298 spectrophotometer in KBr pellets. UV/Vis spectra of 0.01 mmol solutions in 2%DMSO/MeOH or 0.08%DMSO/MeOH were recorded on a Specord 200 spectrometer (Supplementary Materials).

2.2. Synthesis of 7-(4-(5-Amino-1-R-1H-1,2,3-triazole-4-carbonyl)piperazin-1-yl)-1-R-6-fluoro-4-oxo-1,4-dihydroquinoline-3-carboxylic Acid 1b, c, 2d-1 (General Method)

To a solution of quinolone (1a, 2a) (10 mmol) in DMSO (10 mL) and MeOH (5 mL), substituted azide (12 mmol) and sodium methoxide in methanol (30 mmol) were added.

The reaction mixture was refluxed overnight. After completion of the reaction (detected by TLC), the reaction mixture was cooled. Then water was added and the mixture was acidified with 0.1 M HCl. The solid product was collected by filtration, washed with water, and dried and purified by recrystallization with butanol. Yield after recrystallization was 37–68%.

2.2.1. 7-(4-(5-Amino-1-(p-tolyl)-1H-1,2,3-triazole-4-carbonyl)piperazin-1-yl)-1-ethyl-6-fluoro-4-oxo-1,4-dihydroquinoline-3-carboxylic Acid 1b

Yield 0.34 g (65%). Mp 250–255°C. ^1H NMR spectrum ppm, δ 8.54 (s, 1H), 7.84 (d, $J = 13.6$ Hz, 2H), 7.44 (d, $J = 10.5$ Hz, 6H), 7.08 (s, 2H), 6.57 (s, 2H), 4.63 (s, 1H), 4.35 (s, 2H), 3.85 (s, 1H), 2.41 (s, 5H), 1.35 (s, 3H). ^{13}C NMR (100 MHz, DMSO) δ 175.76, 166.65, 161.39, 152.43, 149.98, 147.87, 145.52, 144.76, 137.60, 137.43, 134.35, 130.09, 123.78, 123.47, 120.41, 113.30, 113.07, 109.77, 105.19, 49.64, 49.60, 48.93, 46.48, 21.07, 14.31. LC/MS m/z (I_{rel} , %): 520.1 $[\text{M}+\text{H}]^+$ (100). IR spectrum (KBr), ν , cm^{-1} : 3419 (OH, st), 2923, 2855 (C=C, st), 1622 (C=O carboxylic, st), 1581 (C=O amide, st), 1492 (C=C phenyl, st), 1255 (C-O, st), 1014 (C=C, δ). UV/Vis spectrum (0.08% DMSO/MeOH), λ_{max} nm (ϵ): 280(0.014), 332(0.004). Calc C, 60.11; H, 5.04; F, 3.66; N, 18.87; O, 12.32. Found C, 60.11; H, 5.05; F, 3.67; N, 18.85; O, 12.32.

2.2.2. 7-(4-(5-Amino-1-(4-bromophenyl)-1H-1,2,3-triazole-4-carbonyl)piperazin-1-yl)-1-ethyl-6-fluoro-4-oxo-1,4-dihydroquinoline-3-carboxylic Acid 1c

Yield 0.30 g (58%). Mp 300–304°C. ^1H NMR spectrum ppm, δ 15.34 (s, 1H), 8.96 (s, 1H), 7.96 (d, $J = 13.2$ Hz, 1H), 7–7.58 (m, 2H), 7.52–7.43 (m, 2H), 7.26 (d, $J = 7.2$ Hz, 1H), 6.65 (s, 1H), 4.61 (d, $J = 7.1$ Hz, 2H), 3.44 (s, 2H), 1.43 (t, $J = 7.1$ Hz, 3H). ^{13}C NMR (100 MHz, DMSO) δ 175.76, 166.65, 161.39, 152.16, 149.98, 147.87, 145.52, 144.78, 137.43, 135.36, 132.80, 124.99, 123.78, 120.41, 119.78, 113.30, 113.07, 109.77, 105.14, 49.62, 48.93, 46.48, 14.31. LC/MS m/z (I_{rel} , %): 524.2 $[\text{M}+\text{H}]^+$ (100). IR spectrum (KBr), ν , cm^{-1} : 3400 (OH, st), 2922 (C=C, st), 1628 (C=O carboxylic, st), 1501 (C=O amide, st), 1466, 1447 (C=C phenyl, st), 1256 (C-O, st), 1014 (C=C, δ). UV/Vis spectrum (2% DMSO/MeOH), λ_{max} nm (ϵ): 277(0.051), 314(0.012), 327(0.012). Calc C, 57.36; H, 4.43; F, 7.26; N, 18.73; O, 12.22. Found C, 57.34; H, 4.47; F, 7.28; N, 18.81; O, 12.10.

2.2.3. 7-(4-(5-Amino-1-phenyl-1H-1,2,3-triazole-4-carbonyl)piperazin-1-yl)-1-cyclopropyl-6-fluoro-4-oxo-1,4-dihydroquinoline-3-carboxylic Acid 2d

Yield 0.34 g (66%). Mp 258–260°C. ^1H NMR spectrum ppm, δ 15.20 (s, 1H), 8.67 (s, 1H), 7.94 (d, $J = 13.1$ Hz, 1H), 7.69–7.52 (m, 5H), 6.65 (s, 1H), 4.66 (s, 2H), 3.82 (td, $J = 7.2, 3.7$ Hz, 3H), 3.46 (d, $J = 6.1$ Hz, 4H), 1.39–1.29 (m, 2H), 1.19 (dd, $J = 6.5, 3.9$ Hz, 2H). ^{13}C NMR (101 MHz, DMSO) δ 176.36, 176.33, 165.87, 161.20, 154.22, 151.74, 147.98, 146.86, 146.81, 145.01, 144.91, 139.15, 134.68, 129.81, 129.22, 124.30, 124.28, 121.77, 121.75, 118.85, 118.77, 111.10, 110.88, 106.76, 106.66, 106.62, 49.70, 35.89, 7.58. LC/MS m/z (I_{rel} , %): 518.0 $[\text{M}+\text{H}]^+$ (100). IR spectrum (KBr), ν , cm^{-1} : 3390 (OH, st), 2921, 2854 (C=C, st), 1623 (C=O carboxylic, st), 1512 (C=O amide, st), 1445 (C=C phenyl, st), 1254 (C-O, st), 1014 (C=C, δ). UV/Vis spectrum (0.08% DMSO/MeOH), λ_{max} nm (ϵ): 276(0.082), 312(0.022), 326(0.021). Calc C, 60.34; H, 4.67; F, 3.67; N, 18.95; O, 12.37. Found C, 60.35; H, 4.62; F, 3.70; N, 18.99; O, 12.34.

2.2.4. 7-(4-(5-Amino-1-(2-methylphenyl)-1H-1,2,3-triazole-4-carbonyl)piperazin-1-yl)-1-cyclopropyl-6-fluoro-4-oxo-1,4-dihydroquinoline-3-carboxylic Acid 2e

Yield 0.20 g (37%). Mp 215–220°C. ^1H NMR spectrum ppm ^1H NMR (400 MHz, DMSO- d_6) δ 15.19 (s, 1H), 8.67 (s, 1H), 7.94 (dd, $J = 13.1, 7.0$ Hz, 1H), 7.62 (t, $J = 9.4$ Hz, 1H), 7.58–7.40 (m, 2H), 7.37 (d, $J = 7.8$ Hz, 1H), 6.48 (s, 1H), 4.63 (d, $J = 42.7$ Hz, 2H), 3.83 (s, 4H), 3.47 (s, 3H), 2.54 (s, 2H), 2.07 (s, 2H), 1.35 (q, $J = 6.9$ Hz, 2H), 1.19 (s, 2H). ^{13}C NMR (100 MHz, DMSO) δ 175.67, 165.78, 161.34, 152.56, 150.11, 147.86, 145.61, 144.90, 144.78, 138.81, 136.40, 133.41, 130.69, 130.12, 126.88, 124.25, 123.92, 120.90, 112.88, 112.65, 110.19, 106.65, 106.59, 49.64, 49.60, 46.48, 35.75, 17.35, 8.34. LC/MS m/z (I_{rel} , %): 548.1 $[\text{M}+\text{H}]^+$ (100). IR spectrum (KBr), ν , cm^{-1} : 3427 (OH, st), 2923, 2854 (C=C, st), 1628 (C=O carboxylic, st),

1511 (C=O amide, st), 1470,1447 (C=C phenyl, st), 1256 (C-O, st), 1013 (C=C, δ). UV/Vis spectrum (0.08%DMSO/MeOH), λ_{\max} nm (ϵ): 277 (0.047), 327 (0.011). Calc C, 61.01; H, 4.93; F, 3.57; N, 18.45; O, 12.04. Found C, 61.01; H, 4.96; F, 3.55; N, 18.49; O, 11.99.

2.2.5. 7-(4-(5-Amino-1-(4-ethylphenyl)-1H-1,2,3-triazole-4-carbonyl)piperazin-1-yl)-1-cyclopropyl-6-fluoro-4-oxo-1,4-dihydroquinoline-3-carboxylic Acid 2f

Yield 0.20 g (68%). Mp 258-262C. ^1H NMR spectrum ppm, δ 15.21 (s, 1H), 8.68 (s, 1H), 7.96 (d, J = 13.1 Hz, 1H), 7.63 (d, J = 7.4 Hz, 1H), 7.48 (q, J = 8.4 Hz, 3H), 6.59 (s, 1H), 4.66 (s, 1H), 3.87–3.80 (m, 2H), 3.46 (s, 3H), 2.72 (q, J = 7.6 Hz, 2H), 2.54 (s, 5H), 1.34 (t, J = 6.6 Hz, 2H), 1.29–1.12 (m, 5H). ^{13}C NMR (100 MHz, DMSO) δ 175.67, 165.78, 161.39, 152.56, 150.11, 147.86, 144.90, 144.76, 141.21, 138.81, 134.91, 128.75, 124.53, 123.78, 120.90, 112.88, 112.65, 110.19, 106.65, 106.59, 49.64, 49.60, 46.48, 35.75, 28.14, 15.38, 8.34. LC/MS m/z (I_{rel} , %): 546.2 $[\text{M}+\text{H}]^+$ (100). IR spectrum (KBr), ν , cm^{-1} : 3374 (OH, st), 2960, 2926 (C=C, st), 1619 (C=O carboxylic, st), 1520 (C=O amide, st), 1445 (C=C phenyl, st), 1254 (C-O, st), 1013 (C=C, δ). UV/Vis spectrum (0.08% DMSO/MeOH), λ_{\max} nm (ϵ): 281 (0.078), 318 (0.022), 331 (0.021). Calc C, 61.64; H, 5.17; F, 3.48; N, 17.97; O, 11.73. Found C, 61.64; H, 5.15; F, 3.45; N, 18.00; O, 11.75.

2.2.6. 7-(4-(5-Amino-1-(4-ethylphenyl)-1H-1,2,3-triazole-4-carbonyl)piperazin-1-yl)-1-cyclopropyl-6-fluoro-4-oxo-1,4-dihydroquinoline-3-carboxylic Acid 2g

Yield 0.24 g (43%). Mp 260-262C. ^1H NMR spectrum ppm, δ 15.20 (s, 1H), 8.68 (s, 1H), 7.95 (d, J = 13.1 Hz, 1H), 7.63 (d, J = 7.3 Hz, 1H), 7.53–7.45 (m, 2H), 7.20–7.12 (m, 2H), 6.52 (s, 1H), 4.66 (s, 2H), 3.85 (s, 2H), 3.82 (dd, J = 7.4, 4.0 Hz, 2H), 3.46 (d, J = 6.0 Hz, 3H), 2.54 (s, 4H), 1.34 (d, J = 6.8 Hz, 2H), 1.18 (q, J = 5.7, 4.2 Hz, 2H). ^{13}C NMR (100 MHz, DMSO) δ 175.67, 165.78, 161.39, 159.03, 152.56, 150.11, 147.86, 144.90, 144.78, 144.68, 138.81, 130.70, 126.09, 123.85, 120.90, 115.27, 112.88, 112.65, 110.19, 106.65, 106.59, 55.33, 49.64, 49.60, 46.48, 35.75, 8.34. LC/MS m/z (I_{rel} , %): 548.2 $[\text{M}+\text{H}]^+$ (100). IR spectrum (KBr), ν , cm^{-1} : 3435 (OH, st), 2923, 2855 (C=C, st), 1621 (C=O carboxylic, st), 1523 (C=O amide, st), 1468, 1448 (C=C phenyl, st), 1246 (C-O, st), 1021 (C=C, δ). UV/Vis spectrum (0.08%DMSO/MeOH), λ_{\max} nm (ϵ): 281 (0.145), 318 (0.046), 329 (0.045). Calc C, 59.23; H, 4.79; F, 3.47; N, 17.91; O, 14.61. Found C, 59.20; H, 4.78; F, 3.49; N, 17.98; O, 14.56.

2.2.7. 7-(4-(5-Amino-1-(4-(methylthio)phenyl)-1H-1,2,3-triazole-4-carbonyl)piperazin-1-yl)-1-cyclopropyl-6-fluoro-4-oxo-1,4-dihydroquinoline-3-carboxylic Acid 2h

Yield 0.28 g (49%). Mp 280-285C. ^1H NMR spectrum ppm, δ 15.22 (s, 1H), 8.68 (s, 1H), 7.96 (d, J = 13.2 Hz, 1H), 7.63 (d, J = 7.5 Hz, 1H), 7.50 (q, J = 8.7 Hz, 4H), 6.62 (s, 2H), 4.66 (s, 1H), 3.83 (s, 4H), 3.45 (s, 3H), 1.34 (d, J = 6.7 Hz, 2H), 1.19 (s, 2H). ^{13}C NMR (100 MHz, DMSO) δ 175.67, 165.78, 161.39, 152.56, 150.11, 147.86, 144.90, 144.77, 138.81, 137.25, 134.23, 128.42, 123.78, 123.55, 120.90, 112.88, 112.65, 110.18, 106.65, 106.59, 49.64, 49.60, 46.48, 35.75, 15.49, 8.34. LC/MS m/z (I_{rel} , %): 564.1 $[\text{M}+\text{H}]^+$ (100). IR spectrum (KBr), ν , cm^{-1} : 3445 (OH, st), 2923, 2852 (C=C, st), 1620 (C=O carboxylic, st), 1520 (C=O amide, st), 1469 (C=C phenyl, st), 1256 (C-O, st), 1016 (C=C, δ). UV/Vis spectrum (2%DMSO/MeOH), λ_{\max} nm (ϵ): 281 (0.062), 318 (0.014), 331 (0.013). Calc C, 57.54; H, 4.65; F, 3.37; N, 17.40; O, 11.35; S, 5.69. Found C, 57.50; H, 4.65; F, 3.38; N, 17.47; O, 11.30; S, 5.70.

2.2.8. 7-(4-(5-Amino-1-(3-(methylthio)phenyl)-1H-1,2,3-triazole-4-carbonyl)piperazin-1-yl)-1-cyclopropyl-6-fluoro-4-oxo-1,4-dihydroquinoline-3-carboxylic Acid 2i

Yield 0.32 g (57%). Mp 226-232C. ^1H NMR spectrum ppm, δ 15.20 (s, 1H), 8.68 (s, 1H), 7.95 (d, J = 13.1 Hz, 1H), 7.63 (d, J = 7.4 Hz, 1H), 7.55 (t, J = 7.9 Hz, 1H), 7.44 (d, J = 11.7 Hz, 2H), 7.35 (d, J = 7.9 Hz, 1H), 6.70 (s, 1H), 4.66 (s, 3H), 3.84 (s, 4H), 3.46 (s, 3H), 1.34 (t, J = 6.8 Hz, 2H), 1.19 (s, 2H). ^{13}C NMR (75 MHz, DMSO- d_6) δ 175.67, 165.78, 161.39, 152.56, 147.86, 144.95, 138.81, 138.46, 136.62, 128.73, 125.26, 123.94, 121.43, 121.03, 120.90, 112.88, 112.65, 110.18, 106.65, 49.64, 49.60, 46.48, 35.75, 15.61, 8.34. LC/MS m/z (I_{rel} , %): 564.2 $[\text{M}+\text{H}]^+$ (100). IR spectrum (KBr), ν , cm^{-1} : 3444 (OH, st), 2921, 2852 (C=C, st), 1620 (C=O carboxylic, st), 1507 (C=O amide, st), 1469,1446 (C=C phenyl, st), 1255 (C-O, st), 1016 (C=C,

δ). UV/Vis spectrum (0.08% DMSO/MeOH), λ_{\max} nm (ϵ): 280 (0.016), 316 (0.006). Calc C, C, 57.54; H, 4.65; F, 3.37; N, 17.40; O, 11.35; S, 5.69. Found C, C, 57.54; H, 4.65; F, 3.35; N, 17.90; O, 11.32; S, 5.64.

2.2.9. 7-(4-(5-Amino-1-(4-bromophenyl)-1H-1,2,3-triazole-4-carbonyl)piperazin-1-yl)-1-cyclopropyl-6-fluoro-4-oxo-1,4-dihydroquinoline-3-carboxylic Acid 2j

Yield 0.35 g (61%). Mp 275–280C. ^1H NMR spectrum ppm, δ 15.20 (s, 1H), 8.68 (s, 1H), 7.96 (d, J = 13.0 Hz, 1H), 7.83 (d, J = 8.3 Hz, 2H), 7.63 (d, J = 7.4 Hz, 1H), 7.57 (d, J = 8.3 Hz, 2H), 6.71 (s, 1H), 4.65 (s, 2H), 3.83 (s, 4H), 3.45 (s, 3H), 2.44 (s, 2H), 1.34 (d, J = 7.0 Hz, 2H), 1.19 (s, 2H). ^{13}C NMR (100 MHz, DMSO) δ 175.67, 165.78, 161.39, 152.56, 147.86, 144.78, 138.81, 135.36, 132.80, 124.99, 123.78, 119.78, 112.88, 112.65, 110.18, 106.65, 49.62, 46.48, 35.75, 8.34. LC/MS m/z (I_{rel} , %): 598.1 $[\text{M}+\text{H}]^+$ (100). IR spectrum (KBr), ν , cm^{-1} : 3391 (OH, st), 2920, 2854 (C=C, st), 1627 (C=O carboxylic, st), 1515 (C=O amide, st), 1443 (C=C phenyl, st), 1258 (C-O, st), 1017 (C=C, δ). UV/Vis spectrum (2%DMSO/MeOH), λ_{\max} nm (ϵ): 283 (0.048), 315 (0.012), 331 (0.011). Calc C, 52.36; H, 3.89; Br, 13.40; F, 3.19; N, 16.44; O, 10.73. Found C, 52.35; H, 3.85; Br, 13.42; F, 3.15; N, 16.47; O, 10.77.

2.2.10. 7-(4-(5-Amino-1-(5-fluoro-2-methylphenyl)-1H-1,2,3-triazole-4-carbonyl)piperazin-1-yl)-1-cyclopropyl-6-fluoro-4-oxo-1,4-dihydroquinoline-3-carboxylic Acid 2k

Yield 0.27 g (50%). Mp 278–282C. ^1H NMR spectrum ppm, δ 15.21 (s, 1H), 8.68 (s, 1H), 7.96 (d, J = 13.1 Hz, 1H), 7.63 (d, J = 7.5 Hz, 1H), 7.54 (dd, J = 6.8, 2.5 Hz, 1H), 7.49–7.41 (m, 1H), 7.39 (d, J = 8.8 Hz, 1H), 6.64 (s, 1H), 4.66 (s, 2H), 3.83 (s, 4H), 3.46 (s, 3H), 2.33 (d, J = 2.1 Hz, 3H), 1.34 (d, J = 6.9 Hz, 2H), 1.19 (d, J = 4.5 Hz, 2H). ^{13}C NMR (100 MHz, DMSO) δ 175.67, 165.78, 161.34, 152.56, 147.86, 145.42, 138.81, 131.74, 131.65, 129.18, 124.12, 120.90, 113.63, 113.41, 112.88, 112.65, 110.18, 108.25, 107.99, 106.65, 49.64, 49.60, 46.48, 35.75, 17.46, 8.34. LC/MS m/z (I_{rel} , %): 550.2 $[\text{M}+\text{H}]^+$ (100). IR spectrum (KBr), ν , cm^{-1} : 3393 (OH, st), 2922, 2853 (C=C, st), 1627 (C=O carboxylic, st), 1509 (C=O amide, st), 1470, 1446 (C=C phenyl, st), 1255 (C-O, st), 1020 (C=C, δ). UV/Vis spectrum (0.08% DMSO/MeOH), λ_{\max} nm (ϵ): 281 (0.055), 318 (0.016), 329 (0.015). Calc C, C, 59.01; H, 4.59; F, 6.91; N, 17.84; O, 11.65. Found C, C, 59.01; H, 4.55; F, 6.97; N, 17.88; O, 11.59.

2.2.11. 7-(4-(5-Amino-1-(4-(trifluoromethyl)phenyl)-1H-1,2,3-triazole-4-carbonyl)piperazin-1-yl)-1-cyclopropyl-6-fluoro-4-oxo-1,4-dihydroquinoline-3-carboxylic Acid 2l

Yield 0.29 g (49%). Mp 222–228C. ^1H NMR spectrum ppm, δ 15.14 (s, 1H), 8.67 (s, 1H), 7.99–7.91 (m, 4H), 7.91–7.83 (m, 2H), 7.62 (d, J = 7.3 Hz, 1H), 6.81 (s, 2H), 4.64 (s, 1H), 3.82 (s, 4H), 3.46 (s, 3H), 1.34 (d, J = 5.9 Hz, 2H), 1.18 (s, 2H). ^{13}C NMR (100 MHz, DMSO) δ 175.67, 165.78, 161.39, 152.56, 150.11, 147.86, 144.90, 144.77, 138.81, 135.82, 127.40, 127.08, 123.78, 123.47, 112.88, 112.65, 110.18, 106.60, 40.43, 40.15, 39.87, 39.59, 39.31, 39.04, 38.76, 35.75, 8.34. LC/MS m/z (I_{rel} , %): 586.1 $[\text{M}+\text{H}]^+$ (100). IR spectrum (KBr), ν , cm^{-1} : 3412 (OH, st), 2922, 2853 (C=C, st), 1626 (C=O carboxylic, st), 1508 (C=O amide, st), 1469, 1445 (C=C phenyl, st), 1256 (C-O, st), 1017 (C=C, δ). UV/Vis spectrum (2%DMSO/MeOH), λ_{\max} nm (ϵ): 281 (0.027). Calc C, 55.39; H, 3.96; F, 12.98; N, 16.75; O, 10.93. Found C, 55.35; H, 3.99; F, 12.95; N, 16.80; O, 10.92.

2.3. Docking Studies

The software package for docking studies was the same as in our previous studies [26,27], namely: AutoDock 4.2; MGL Tools 1.5.6 program; Avogadro program, Discovery Studio Visualizer program. The output formats of the receptor and ligand data were converted to a PDBQT format. The antibacterial targets were as follows: *Staphylococcus aureus* DNA Gyrase PDB ID: 2XCR; *Mycobacterium tuberculosis* topoisomerase II PDB ID:5BTL; *Streptococcus pneumoniae* topoisomerase IV PDB ID: 4KPF from the Protein Data Bank (PDB). The same docking parameters were determined as in our previous paper.

Type IIA topoisomerases cleave and repair DNA to regulate DNA topology and are a major target for antibacterials, but do not have a well-developed structural basis for understanding the mechanism of action of the medicine. Recent studies have reported a crystalline structure of a new class of broad-spectrum antibacterial agents in combination with DNA gyrase and *Staphylococcus aureus* DNA, demonstrating a new method of inhibition that bypasses fluoroquinolone resistance in this clinically important drug target. The inhibitor connects DNA and a temporary non-catalytic double-axis pocket on the GyrA dimeric region, which is located close to the active sites and binding sites of fluoroquinolone. In the inhibitor complex, the active site appears to be ready to cleave DNA with a single metal ion located between the TOPRIM domain (topoisomerase/primase) and the cleaving phosphate. This development gives a new idea on the new mechanisms of action and the possibility of creating a platform for the design of medicines based on the structures of a new class of antibacterial agents, relative to the clinically tested and conformationally flexible class of enzymes [28].

Fluoroquinolone antibacterials have DNA gyrase as a target and are critical agents used to stop the progression of multidrug-resistant tuberculosis; however, resistance to fluoroquinolones is constantly increasing, and new ways to circumvent resistance are needed. Analysis of the structure of complexes in the range from 2.4 to 2.6 Å shows that the truly low susceptibility of *Mycobacterium tuberculosis* (Mtb) to fluoroquinolones correlates with a decrease in contacts involved in additional stabilization of the target molecule complex through the overlapping cation Mg^{2+} interaction of fluoroquinolone and gyrase.

Stability analysis using purified components showed a clear relationship between the reversibility of the ternary complex and the inhibitory activity reported with cultured cells. Taken together, the data obtained indicate that the stability of the fluoroquinolone/DNA interaction is a major determinant of fluoroquinolone activity and that the fragments added to the C-7 position of the various quinolone scaffolds have no advantage in contacting the enzyme. These concepts point to new approaches to the development of quinolone class compounds that have increased efficacy against Mtb and the ability to overcome resistance [29].

As part of the synthesis program and study of biological properties of new antibacterial agents from the group of fluoroquinolones and their focus on topoisomerase IV *Streptococcus pneumoniae*—a crystallographic model of complexes with 7,8-substituted fluoroquinolones (with limited content of C-7) was selected in complex with topoisomerase IV *S. pneumoniae*, with the DNA binding site, consisting of 18 common pairs—E-site [30].

All selected crystallographic models contain ligands based on the quinoline framework, which will predetermine the emergence of affinity for the studied molecules in this series.

2.4. Antibacterial Activity

2.4.1. Method of Double Serial Dilutions

The macro method of double serial dilutions [31,32] was used in the course of the study, which is regulated by EUCAST (v11.0 2021) and the international standard ISO 20776-1: 2006 “Clinical laboratory testing and in vitro diagnostic test systems—Susceptibility testing of infectious agents and evaluation of performance of antimicrobial susceptibility test devices—Part 1: Reference method for testing the in vitro activity of antimicrobial agents against rapidly growing aerobic bacteria involved in infectious diseases”).

Solutions of the synthesized compounds in DMF were prepared at a concentration of 1 mg/mL.

According to WHO recommendations, the following test strains were used: *Staphylococcus aureus* ATCC 25923, *Escherichia coli* ATCC 25922, *Bacillus subtilis* ATCC 6633, *Pseudomonas aeruginosa* ATCC 27853, *Candida albicans* NCTC 885-653.

The antimicrobial properties were studied by performing two dilutions of test samples in 2 mL of meat peptone broth (MPB medium №1) (a total of 10 tubes). A separate pipette was used for each dilution. After that, 0.2 mL of microbial suspension of each test strain

with the appropriate number of microbial cells was added to each tube. For inoculation, a microbial suspension equivalent to 0.5, according to the McFarland standard, diluted 100 times in nutrient broth, was used. Afterward, the concentration of the microorganism in it, approximately 10 CFU/cc. 0.5 cc of inoculum, was added to each tube containing 0.5 cc of test samples of appropriate dilutions, and in one tube of 0.5 cc of nutrient broth, without test substances as a 'negative control'. The final concentration of the microorganism in each tube will reach the required—approximately 5×10 CFU/cc. The inoculum should be introduced into test tubes with dilutions of the test samples no later than 15 min from the moment of its preparation.

Additionally, the control was prepared: 2 tubes with 2 mL of used medium in each—control of medium; 2 tubes with 2 mL of used medium with 0.2 mL of microbial suspension of each test strain—growth control of test microorganisms.

The tubes were placed in a thermostat for 18–24 h. The results were determined visually by the presence or absence of turbidity. The concentration of the compound in the last tube with a clear medium (not visible to the naked eye growth of the test strain) corresponded to the MIC. The control of the test microorganism growth should be observed; medium control must be sterile.

Evaluation of the results determined that the presence of microorganism growth was performed visually according to EUCAST and ISO 20776-1:2006, examining tubes with cultures in transmitted light.

Experiments with *C. albicans* were performed by double dilution of test samples in 2 mL of dextrose broth Sabouraud (a total of 10 tubes). A separate pipette was used for each dilution. After that, 0.2 mL of the microbial suspension of the test strain with the appropriate number of microbial cells was added to each tube. Additionally, the control was prepared: 2 tubes with 2 mL of used medium in each—control of medium; 2 tubes with 2 mL of used medium with 0.2 mL of suspension of the test strain—growth control.

The tubes were placed in a thermostat for 18–24 h. The results were determined visually by the presence or absence of turbidity. The concentration of the compound in the last tube with a clear medium (no visible to the naked eye growth of the test strain) corresponded to the MIC. The control of the growth should be observed; medium control must be sterile. The obtained data were analyzed by variation statistics. The significance level $p \leq 0.05$ was accepted.

2.4.2. Agar Diffusion Method

The antimicrobial activity of the compounds synthesized was studied in vitro by the method of diffusion into agar (the method of wells), the principle of which was to measure the zone of growth retardation of microorganisms [31,32].

The antimicrobial activity was determined immediately after preparation of samples. The studies were performed under aseptic conditions. Pure reference cultures were used as test cultures: Gram-positive culture of *Staphylococcus aureus* ATCC 25923, as well as Gram-negative culture of *Escherichia coli* ATCC 25922 and culture of yeast-like fungi *Candida albicans* ATCC 885-653. In addition, clinical strains of *Staphylococcus aureus*, *Escherichia coli*, and *Candida albicans* were used in the experiment.

One-day suspensions of bacterial microorganisms in physiological solution were used. The microbial load was 107 microbial cells in 1 mL of nutrient medium. Molten agar gel (bottom layer, V = 10 mL) was used as the non-inoculated medium for the Petri dishes mounted on a horizontal surface, and meat-peptone agar (V = 14–15 mL) was used as the inoculated medium. Sterile metal thin-walled cylinders (diameter— 8.0 ± 0.1 mm, height— 10.0 ± 0.1 mm) were used to form the holes. Prior to introduction into the wells, the test substances were dissolved in dimethyl sulfoxide (DMSO).

The results were recorded by measuring the growth retardation zone of microorganisms. Measurements were performed with an accuracy of 1 mm, focusing on the complete absence of visible growth. The value of the zone of growth retardation of pure DMSO was subtracted from the results of the analyses of the model samples. The antimicrobial activity

of experimental samples was evaluated by the diameter of the growth retardation zone of microorganisms: sample; growth retardation zones with a diameter of 11–15 mm were evaluated as low sensitivity of the culture to the concentration of the active antimicrobial substance; zones of growth retardation with a diameter of 16–25 mm—as an indicator of the sensitivity of the strain of the microorganism to the test sample; the growth retardation zone, the diameter of which exceeded 25 mm, indicates a high sensitivity of microorganisms.

3. Results

3.1. Synthesis

Previous investigations of our scientific team [33] resulted in the creation of an effective one-step procedure towards novel 7-(4-(2-cyanoacetyl)piperazin-1-yl)-1-R-6-fluoro-4-oxo-1,4-dihydroquinoline-3-carboxylic acids **1a**, **2a** (Figure 2).

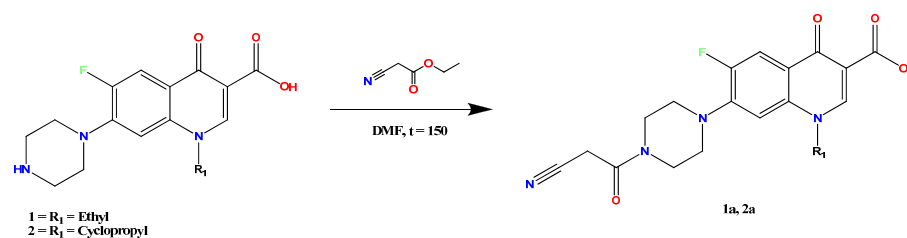


Figure 2. Synthesis of 7-(4-(2-cyanoacetyl)piperazin-1-yl)-1-R-6-fluoro-4-oxo-1,4-dihydroquinoline-3-carboxylic acids **1a**, **2a**.

This reaction can proceed both in DMF solution and without it. However, the first option gave the target products with higher purity and better yield. Moreover, the two-step approach is possible utilizing cyanoacetic and CDI to synthesize intermediate N-(cyanoacetyl)imidazole for the reaction with starting fluoroquinolones. However, according to the obtained results, the one-step procedure depicted above appeared to be much more suitable.

Continuing this investigation, first, we synthesized substituted azides according to known methods [34]. Secondly, they were utilized under traditional reaction conditions with sodium methoxide as a catalyst in reactions with 7-(4-(2-cyanoacetyl)piperazin-1-yl)-1-R-6-fluoro-4-oxo-1,4-dihydroquinoline-3-carboxylic acids **1a**, **2a** (Figure 3).

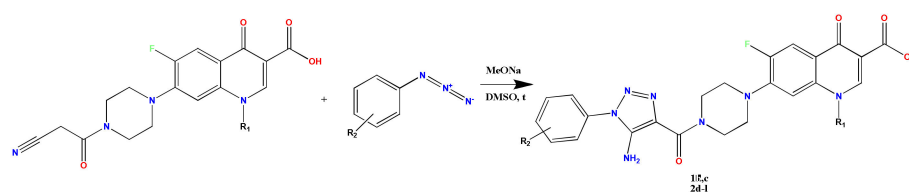


Figure 3. Synthesis of the target compounds.

According to the described procedure, novel norfloxacin and ciprofloxacin derivatives **1b,c**, **2d-l** were successfully obtained with 37–68% yield and their structures were confirmed by ¹H NMR, ¹³C NMR, ¹⁹F NMR, LC/MS, UV-, IR- spectroscopy (Table 1).

Table 1. Melting points, elemental analyses, and yields for compounds **1b,c, 2d-l**.

Compound Number	R ₂	M.p., °C	Molecular Formula, M. w.	Yield, %
1b	p-Me	250–255	C ₂₆ H ₂₆ FN ₇ O ₄ 519.54	65
1c	p-Br	300–304	C ₂₅ H ₂₃ BrFN ₇ O ₄ 523.49	58
2d	H	258–260	C ₂₆ H ₂₄ FN ₇ O ₄ 517.52	66
2e	o-Me	215–220	C ₂₇ H ₂₆ FN ₇ O ₄ 531.54	37
2f	p-Et	258–262	C ₂₈ H ₂₈ FN ₇ O ₄ 545.58	68
2g	p-OMe	260–262	C ₂₇ H ₂₆ FN ₇ O ₅ 547.55	43
2h	p-SMe	280–285	C ₂₇ H ₂₆ FN ₇ O ₄ S 563.62	49
2i	m-SMe	226–232	C ₂₇ H ₂₆ FN ₇ O ₄ S 563.62	57
2j	p-Br	275–280	C ₂₆ H ₂₃ BrFN ₇ O ₄ 596.42	61
2k	2-Me-5-F	278–282	C ₂₇ H ₂₅ F ₂ N ₇ O ₄ 549.54	50
2l	p-CF ₃	222–228	C ₂₇ H ₂₃ F ₄ N ₇ O ₄ 585.52	49

3.2. Docking Studies

Based on the results of the molecular docking, we calculated the scoring function, indicating the enthalpy contribution to the value of the free binding energy (Affinity DG) for the best conformation positions; the values of the free binding energy and binding constants (EDoc kcal/mol and Ki (uM micromolar) for a definite conformational position of the ligand, which allowed us to evaluate the stability of complexes formed between ligands and the corresponding targets (Table 2). The thermodynamic probability of such binding is confirmed by the negative values of the scoring functions.

3.3. Antibacterial Activity Evaluation

Investigation of the synthesized compounds antimicrobial activity at the first stage was performed in vitro against next test strains of bacterial and fungal cultures: *Staphylococcus aureus* ATCC 25923, *Escherichia coli* ATCC 25922, *Bacillus subtilis* ATCC 6633, *Pseudomonas aeruginosa* ATCC 27853, *Candida albicans* NCTC 885-653.

The method of double serial dilution was used in the study. Solutions of the synthesized compounds in DMF were prepared at a concentration of 1 mg/mL.

According to the obtained results, the compound **2d** (Figure 4) showed a rather wide range of bactericidal activity against all tested test strains (MIC = 15.6 µg/mL). The activity of other compounds was at the control level (MIC = 125 µg/mL).

Table 2. The values of affinity DG, free binding energy, and binding coefficients for the best conformational positions of the test compounds in combination with biotargets (PDB ID: 2XCR, 5BTL, 4KPF).

Molecule	2XCR			5BTL			4KPF		
	Affinity DG, kcal/mol	EDoc kcal/mol	Ki μ M Micromolar	Affinity DG, kcal/mol	EDoc kcal/mol	Ki μ M Micromolar	Affinity DG, kcal/mol	EDoc kcal/mol	Ki μ M Micromolar
1b	−9.4	−4.96	233.07 μ M	−9.0	−4.90	255.07 μ M	−9.5	−4.30	700.35 μ M
1c	−9.4	−5.25	141.96 μ M	−10.8	−5.08	187.55 μ M	−9.1	−4.77	316.56 μ M
2d	−9.8	−4.16	891.54 μ M	−8.6	−5.24	144.69 μ M	−9.3	−4.45	547.64 μ M
2e	−9.6	−4.51	498.52 μ M	−10.6	−6.51	16.79 μ M	−9.6	−5.03	204.77 μ M
2f	−10.4	−4.96	230.68 μ M	−8.7	−5.06	195.51 μ M	−9.1	−4.73	341.42 μ M
2g	−9.8	−5.54	87.25 μ M	−9.6	−4.41	581.77 μ M	−9.2	−4.13	934.16 μ M
2h	−9.1	−5.66	70.49 μ M	−8.8	−4.90	256.42 μ M	−9.2	−4.65	388.76 μ M
2i	−9.3	−4.78	312.12 μ M	−8.7	−5.32	125.18 μ M	−9.0	−4.69	366.76 μ M
2j	−9.6	−4.60	423.83 μ M	−9.5	−5.16	165.25 μ M	−8.4	−4.01	1150 μ M
2k	−9.8	−5.05	197.24 μ M	−9.4	−5.45	101.76 μ M	−8.5	−4.00	1170 μ M
2l	−9.9	−5.24	144.73 μ M	−8.8	−5.92	45.87 μ M	−9.7	−3.99	1191 μ M
Ciprofloxacin	−7.2	−5.10	183.79 μ M	−7.5	−5.51	91.69 μ M	−7.4	−5.38	113.52 μ M
Norfloxacin	−7.2	−4.30	708.28 μ M	−7.8	−5.25	142.92 μ M	−7.4	−4.78	315.73 μ M

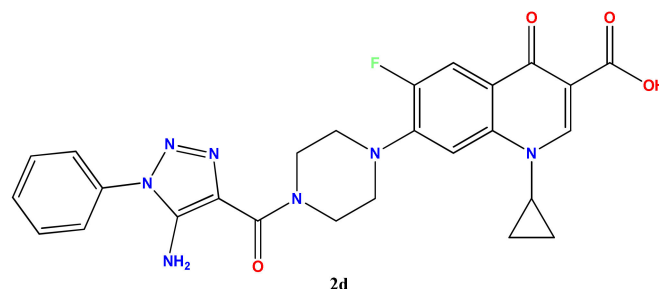


Figure 4. Compound 2d with the highest level of antibacterial activity.

As a continuation of this research, we decided to check the synthesized molecule potency utilizing the diffusion in agar method and hospital strains. The results against reference and clinical strains of *S. aureus* and *E. coli* are represented in Table 3. Growth retardation zone exceeded 25 mm, which corresponds to the high sensitivity of microorganisms towards the tested compounds.

Table 3. Activity of the synthesized compounds measured by the agar diffusion method.

Compound	Growth Retardation Zone, mm					
	Reference Strains			Clinical Strains		
	<i>S. aureus</i> ATCC 25923	<i>E. coli</i> ATCC 25922	<i>C. albicans</i> ATCC 885-653	<i>S. aureus</i>	<i>E. coli</i>	<i>C. albicans</i>
1b	34.3 ± 1.8 <i>p</i> = 0.0089	23.8 ± 1.6 <i>p</i> = 0.7521	30.1 ± 1.5 <i>p</i> = 0.0030	25.8 ± 1.4 <i>p</i> = 0.5903	18.7 ± 1.2 <i>p</i> = 0.0569	24.6 ± 1.5 <i>p</i> = 0.1984
1c	34.4 ± 1.4 <i>p</i> = 0.0044	40.4 ± 1.9 <i>p</i> = 0.0008	17.1 ± 1.8 <i>p</i> = 0.2443	27.9 ± 1.7 <i>p</i> = 0.2495	29.3 ± 1.5 <i>p</i> = 0.1185	14.7 ± 1.2 <i>p</i> = 0.0298
2d	28.8 ± 1.9 <i>p</i> = 0.2158	26.5 ± 1.8 <i>p</i> = 0.5553	25.1 ± 1.3 <i>p</i> = 0.0720	24.4 ± 1.7 <i>p</i> = 0.9736	22.3 ± 1.5 <i>p</i> = 0.4811	19.4 ± 1.4 <i>p</i> = 0.5773
2e	33.1 ± 1.8 <i>p</i> = 0.0171	33.4 ± 1.4 <i>p</i> = 0.0075	16.8 ± 1.3 <i>p</i> = 0.1367	27.6 ± 1.7 <i>p</i> = 0.2886	27.4 ± 1.7 <i>p</i> = 0.3458	18.2 ± 1.4 <i>p</i> = 0.3242
2f	36.1 ± 1.7 <i>p</i> = 0.0028	35.4 ± 1.7 <i>p</i> = 0.0038	15.8 ± 1.4 <i>p</i> = 0.0758	28.8 ± 1.7 <i>p</i> = 0.1574	26.3 ± 1.9 <i>p</i> = 0.5665	13.2 ± 1.3 <i>p</i> = 0.0123
2g	35.7 ± 1.8 <i>p</i> = 0.0042	35.4 ± 1.4 <i>p</i> = 0.0021	22.4 ± 1.3 <i>p</i> = 0.4254	26.4 ± 1.3 0.4416	29.6 ± 1.5 <i>p</i> = 0.1001	19.6 ± 1.8 <i>p</i> = 0.6688
2h	36.3 ± 2.6 <i>p</i> = 0.0108	29.3 ± 1.4 <i>p</i> = 0.1077	20.7 ± 1.9 <i>p</i> = 0.9454	30.3 ± 1.6 <i>p</i> = 0.0622	22.3 ± 1.7 <i>p</i> = 0.5044	18.7 ± 1.6 <i>p</i> = 0.4457
2i	29.2 ± 1.5 <i>p</i> = 0.1121	32.2 ± 1.3 <i>p</i> = 0.0140	16.6 ± 2.2 <i>p</i> = 0.2446	25.3 ± 1.6 <i>p</i> = 0.7338	20.1 ± 1.4 <i>p</i> = 0.1547	11.5 ± 1.2 <i>p</i> = 0.0033
2j	35.7 ± 1.67 <i>p</i> = 0.0034	28.9 ± 1.7 <i>p</i> = 0.1726	16.3 ± 1.7 <i>p</i> = 0.1150	29.2 ± 1.8 <i>p</i> = 0.1372	21.2 ± 1.6 <i>p</i> = 0.2786	13.1 ± 1.3 <i>p</i> = 0.0115
2k	33.8 ± 1.4 <i>p</i> = 0.0064	42.7 ± 2.1 <i>p</i> = 0.00001	18.3 ± 1.6 <i>p</i> = 0.4096	27.3 ± 1.3 <i>p</i> = 0.2790	33.4 ± 1.3 <i>p</i> = 0.0079	16.4 ± 1.7 <i>p</i> = 0.1466
2l	17.5 ± 1.8 <i>p</i> = 0.0572	32.3 ± 1.6 <i>p</i> = 0.0207	18.6 ± 1.8 <i>p</i> = 0.5051	14.1 ± 1.4 <i>p</i> = 0.0036	21.8 ± 1.6 <i>p</i> = 0.3987	13.1 ± 1.1 <i>p</i> = 0.0083
Control	24.2 ± 1.8	24.7 ± 1.6	20.5 ± 1.34	24.3 ± 1.7	24.4 ± 1.8	20.9 ± 1.6

Note. *p*—level of significance of differences from control (Student's *t*-test for independent variables).

4. Discussion

Existing fluoroquinolones possess several positions in their structures that can be easily modified from the chemical viewpoint. Such modifications lead to changes in pharmacokinetics and pharmacodynamics of the starting molecules, as previously shown by authors [4–6].

We introduced a substituent (nitrogen based heterocyclic 1,2,3-triazole moiety) at C-7 of norfloxacin and ciprofloxacin, this position is very important for the interaction with enzyme DNA gyrase and, therefore, for the biological activity of the molecule according to the structure–activity relationship studies [13].

Moreover, *in vitro* investigations of antibacterial activity of earlier synthesized 7-(4-(2-cyanoacetyl)piperazin-1-yl)-1-R-6-fluoro-4-oxo-1,4-dihydroquinoline-3-carboxylic acids revealed the potency of these scaffolds. Together with docking studies, such results led us to the idea of further research in this direction, namely, inserting of heterocyclic moiety at C-7 of norfloxacin and ciprofloxacin.

The synthetic approach was chosen because of the suitability of ‘click chemistry’ concept particularly for substituted 1,2,3-triazoles synthesis [35] and resulted in target 7-(4-(5-amino-1-R-1H-1,2,3-triazole-4-carbonyl)piperazin-1-yl)-1-R-6-fluoro-4-oxo-1,4-dihydroquinoline-3-carboxylic acids with moderate yields.

As can be seen from the obtained docking results, scoring functions do not always correlate with the values of free energies and binding constants. Among the tested molecules, the leader compound with respect to *Staphylococcus aureus* PDB gyrase DNA ID: 2XCR is molecule **2h** with EDoc values of -5.66 kcal/mol, Affinity DG -9.1 kcal/mol, Ki 70.49 μ M micromolar. The leader in relation to topoisomerase II *Mycobacterium tuberculosis* PDB ID: 5BTL is molecule **2l** with EDoc values of -5.92 kcal/mol, Affinity DG -8.8 kcal/mol, Ki 45.87 μ M micromolar. Prior to *Streptococcus pneumoniae* topoisomerase IV, the most active compound is molecule **2f** with EDoc values of -4.73 kcal/mol, Affinity DG -9.1 kcal/mol, Ki 341.42 μ M micromolar. According to the results, it was also found that in all of the calculated values of the studied molecules exceed the reference medicine ciprofloxacin (Table 2).

Altogether, the improvement of affinity, according to the docking studies, can be obtained by the preservation of the fluorine atom in the sixth position and the piperazine system in the seventh position with subsequent substitution by the 1,2,3-triazole ring, additional saturation of molecules, with both donor and acceptor substituents in the aryl molecular moiety.

The next stage of molecular docking was a detailed analysis of the geometric location of the compounds in the active sites of selected topoisomerases, in order to provide a full understanding of the molecules fragments that are involved in binding to biotargets, to get clear guidelines for the rational design of future antibacterials.

The bond between the fluorine atom at the 6-position of the quinoline framework and the amino acid residue of glutamine Glu561 promotes the formation of the complex of molecule **2h** with the DNA gyrase of *Staphylococcus aureus*. The glutamine residue additionally stabilizes the complex with the quinoline cycle due to the π -anionic interaction. The formation of hydrogen bonds is facilitated by the presence of oxygen and hydrogen atoms of the carboxyl group in the 3-position of the quinoline cycle and the amino acid residues of arginine Arg517, glycine Gln541, and alanine Ala540, respectively. The aspartic acid residue Asp643 forms a π -amide bond with the aryl moiety. The quinoline framework is also involved in the formation of the π - π bond with the Tyr557 tyrosine fragment. Alkyl interactions contribute to additional stabilization of the complex among the methyl sulfonyl substituent, phenyl moiety, and lysine residue Lys564 (Figure 5).

The formation of molecule **2l** complex with *Mycobacterium tuberculosis* topoisomerase II is facilitated by hydrogen bonds that occur between the oxygen atoms of the carboxyl group in position 3, and the carbonyl group in position 4 of the quinoline framework, with arginine residues Arg98 and lysine Lys49, respectively. Hydrogen bonds are also formed between the carbonyl linker, which binds 1,2,3-triazole and piperazine rings, the Nitrogen atom of the 1,2,3-triazole moiety to the amino acid residues histidine His85, serine Ser91, His87, and Asp586, respectively (Figure 6).

Fluorine atoms form hydrogen and halogen bonds with amino acid residues Lys484, Asp 586, Glu459. Hydrocarbon bond and Alk interaction occur due to the piperazine ring

and serine residues Ser91 and valine Val51. π -Anionic and π - π interactions are formed in the presence of 1,2,3-triazole and phenyl nuclei with His87.

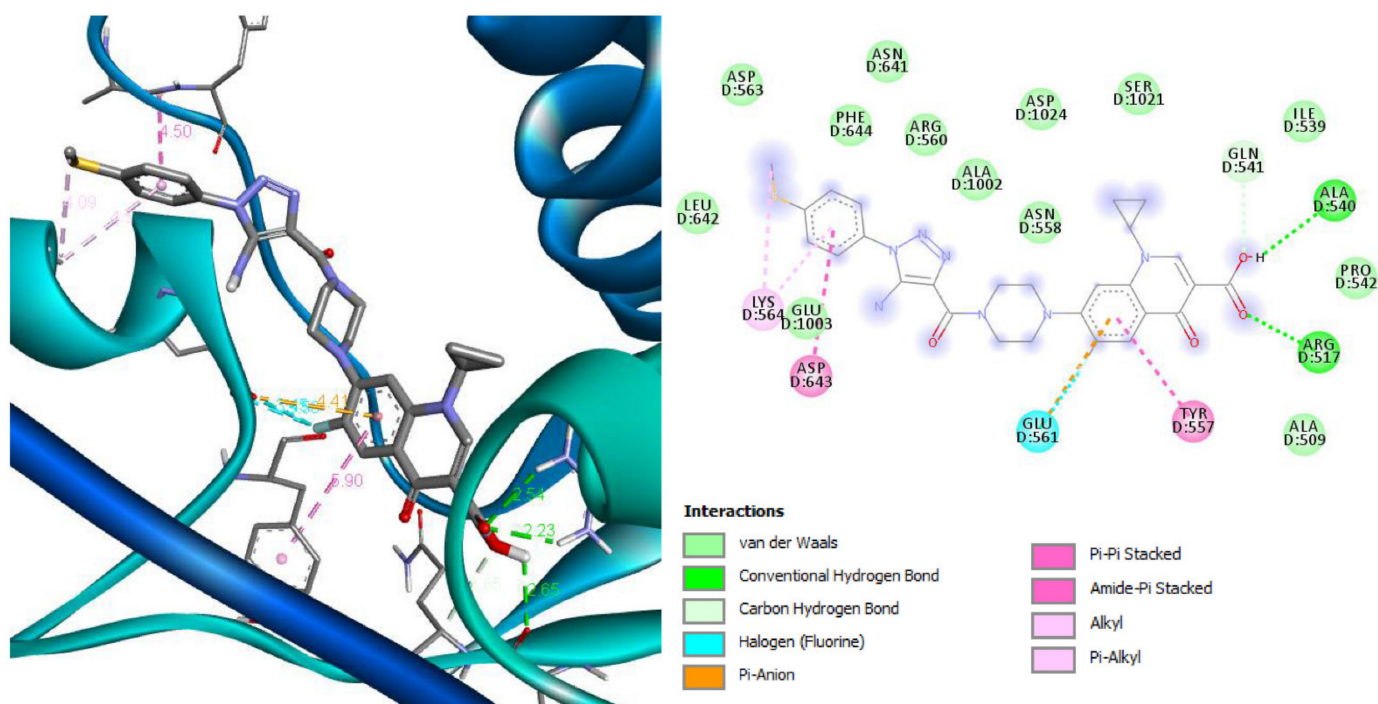


Figure 5. Superposition of compound **2h** and diagram of intermolecular interactions in complex with DNA gyrase *Staphylococcus aureus* (PDB ID: 2XCR).

The complex of molecule **2f** with topoisomerase IV *Streptococcus pneumoniae* is formed with the participation of the fluorine atom in the 6-position of the quinoline cycle and the glycine residue Gln90 in the form of a halogen bond. Hydrogen bonds are formed in the presence of oxygen atoms of the carboxyl group and carbonyl in the third and fourth positions of the quinoline ring with amino acid residues Asn264, Ser107, Trp92. Hydrogen bonding is also observed between the proton of the amino group of the 1,2,3-triazole ring with a serine fragment of Ser80. Hydrocarbon binding occurs between the piperazine ring and the aspartic acid fragment Asp93.

Intermolecular π -cationic and π - σ interactions are formed between the quinoline framework and the phenyl fragment with Lys93 and Val40 residues. π -Alk and Alk interactions between the alkyl group and the 1,2,3-triazole ring with Ala84, Val40, Arg28, His74, and Pro99 residues contribute to additional stabilization (Figure 7).

Given the detailed analysis of the geometric location in the binding sites, the formations between them of a number of intermolecular interactions, negative values of scoring functions, free binding energy, and calculated values of binding constants, we conclude that the studied molecules have affinity to selected biotargets (PDB ID: 2XCR, 5BTL, 4KPF).

This fact was proven by the antibacterial activity investigations, which have shown high sensitivity of microorganisms toward the tested compounds.

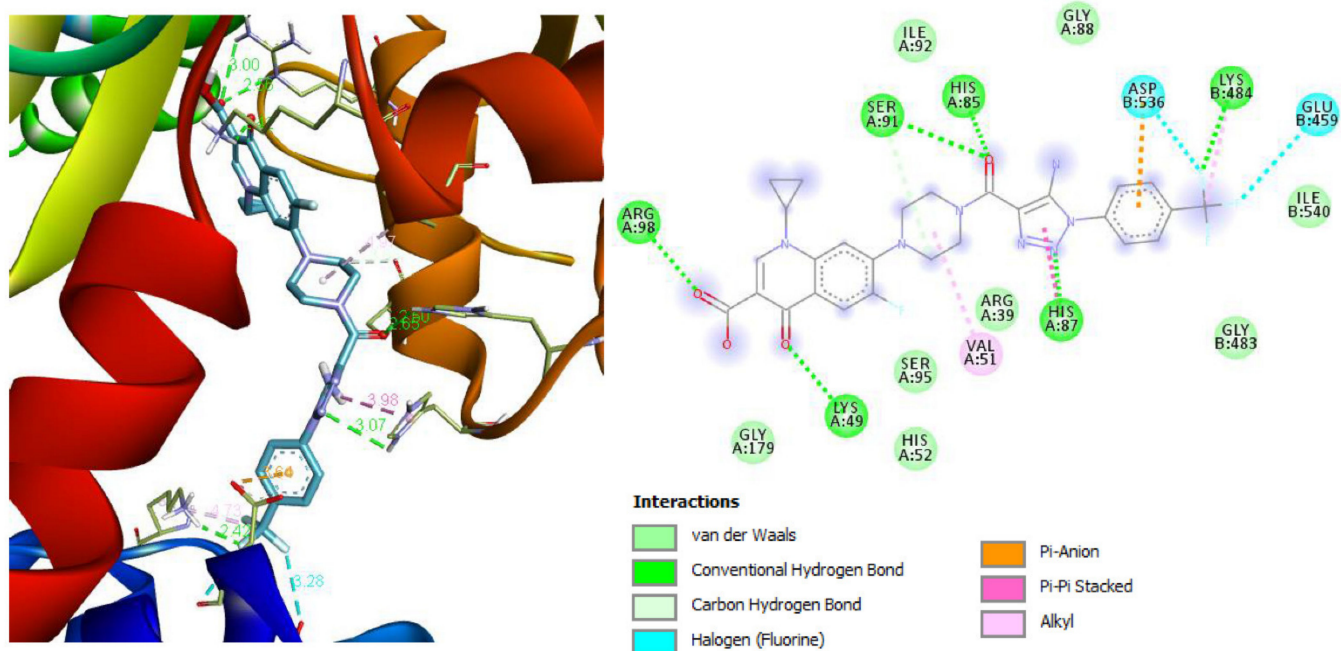


Figure 6. Superposition of molecule 2l and diagram of intermolecular interactions in complex with topoisomerase II *Mycobacterium tuberculosis* (Mtb) (PDB ID:5BTL).

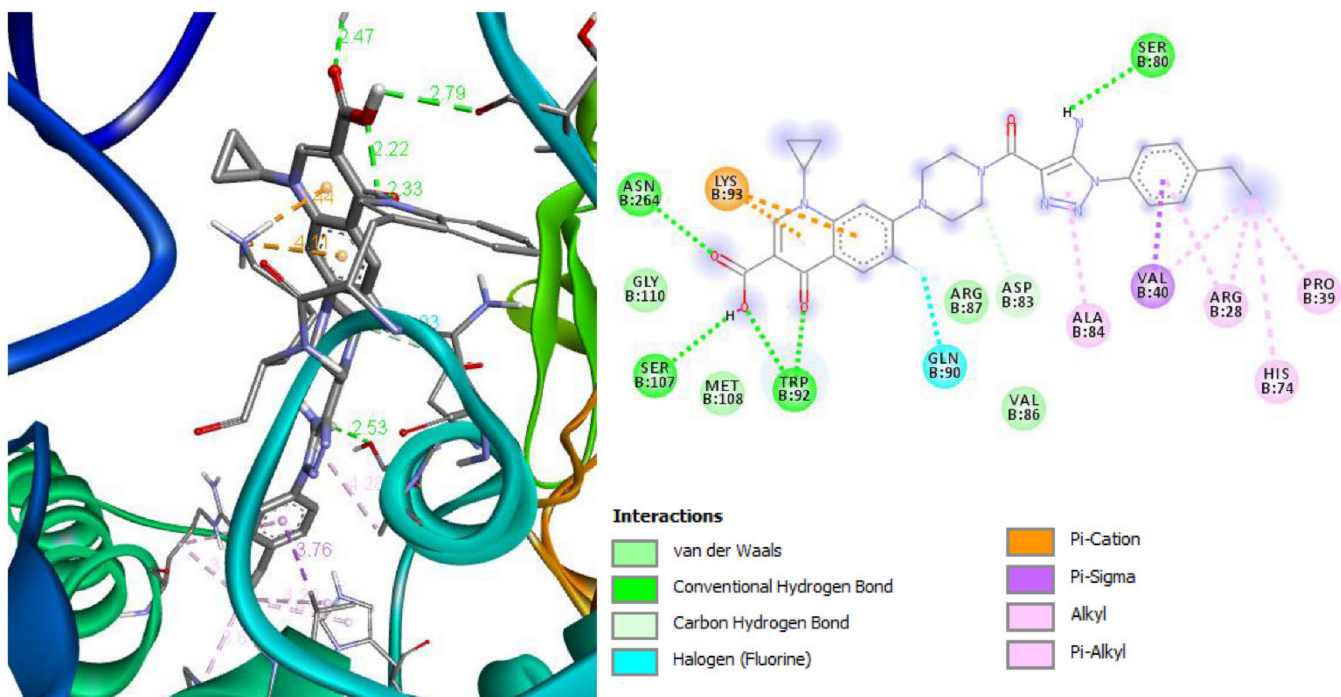


Figure 7. Superposition of molecule 2f and diagram of intermolecular interactions in complex with topoisomerase IV *Streptococcus pneumoniae* (PDB ID: 4KPF).

5. Conclusions

Novel ciprofloxacin and norfloxacin hybrid derivatives were synthesized and their biological activities were investigated in silico and in vitro. The structure and purity of the obtained compounds were confirmed by ¹H NMR, ¹³C NMR, ¹⁹F NMR, LC/MS, UV-, and IR- spectroscopy.

The molecular docking studies for the obtained hybrid compounds showed affinity on the level of ciprofloxacin and norfloxacin. The obtained data contributed to the rational design of novel antibacterials, namely the important structural moieties were revealed:

- Quinoline heterocycle and a fluorine atom in position 6;
- Carbonyl and carboxyl fragments in the third and fourth positions of quinoline, which are involved in additional stabilization of the target molecule complex through the Mg^{2+} cation;
- Substitution in the seventh position of the quinoline framework by pharmacophores of heterocyclic and aromatic structures (triazole, piperazine, and phenyl fragments);
- Additional saturation of molecules with donor and acceptor substituents in the aromatic inclusions of the designed molecules also enhance the activity.

The antibacterial activity research showed antimicrobial and antifungal activities at the reference level for the double dilution method and exceeded control for the agar well diffusion method.

The obtained results appeared to be prospective in the course of new antimicrobial creation.

Supplementary Materials: The following supporting information can be downloaded at: <https://www.mdpi.com/article/10.3390/scipharm90010002/s1>, Figure S1. ¹H NMR spectrum (400 MHz, DMSO-d₆) of 7-(4-(2-cyanoacetyl)piperazin-1-yl)-1-ethyl-6-fluoro-4-oxo-1,4-dihydroquinoline-3-carboxylic acid 1a; Figure S2. ¹³C NMR spectrum (100 MHz, DMSO-d₆) of 7-(4-(2-cyanoacetyl)piperazin-1-yl)-1-ethyl-6-fluoro-4-oxo-1,4-dihydroquinoline-3-carboxylic acid 1a; Figure S3. ¹⁹F NMR spectrum (376 MHz, DMSO-d₆) of 7-(4-(2-cyanoacetyl)piperazin-1-yl)-1-ethyl-6-fluoro-4-oxo-1,4-dihydroquinoline-3-carboxylic acid 1a; Figure S4. LC/MS data for 7-(4-(2-cyanoacetyl)piperazin-1-yl)-1-ethyl-6-fluoro-4-oxo-1,4-dihydroquinoline-3-carboxylic acid 1a; Figure S5. IR spectrum of 7-(4-(2-cyanoacetyl)piperazin-1-yl)-1-ethyl-6-fluoro-4-oxo-1,4-dihydroquinoline-3-carboxylic acid 1a; Figure S6. UV/Vis spectrum of 7-(4-(2-cyanoacetyl)piperazin-1-yl)-1-ethyl-6-fluoro-4-oxo-1,4-dihydroquinoline-3-carboxylic acid 1a; Figure S7. ¹H NMR spectrum (400 MHz, DMSO-d₆) of 7-(4-(2-cyanoacetyl)piperazin-1-yl)-1-cyclopropyl-6-fluoro-4-oxo-1,4-dihydroquinoline-3-carboxylic acid 2a; Figure S8. ¹³C NMR spectrum (100 MHz, DMSO-d₆) of 7-(4-(2-cyanoacetyl)piperazin-1-yl)-1-cyclopropyl-6-fluoro-4-oxo-1,4-dihydroquinoline-3-carboxylic acid 2a; Figure S9. ¹⁹F NMR spectrum (376 MHz, DMSO-d₆) of 7-(4-(2-cyanoacetyl)piperazin-1-yl)-1-cyclopropyl-6-fluoro-4-oxo-1,4-dihydroquinoline-3-carboxylic acid 2a; Figure S10. LC/MS data for 7-(4-(2-cyanoacetyl)piperazin-1-yl)-1-cyclopropyl-6-fluoro-4-oxo-1,4-dihydroquinoline-3-carboxylic acid 2a; Figure S11. IR spectrum of 7-(4-(2-cyanoacetyl)piperazin-1-yl)-1-cyclopropyl-6-fluoro-4-oxo-1,4-dihydroquinoline-3-carboxylic acid 2a; Figure S12. UV/Vis spectrum of 7-(4-(2-cyanoacetyl)piperazin-1-yl)-1-cyclopropyl-6-fluoro-4-oxo-1,4-dihydroquinoline-3-carboxylic acid 2a; Figure S13. ¹H NMR spectrum (400 MHz, DMSO-d₆) of 7-(4-(5-amino-1-(p-tolyl)-1H-1,2,3-triazole-4-carbonyl)piperazin-1-yl)-1-ethyl-6-fluoro-4-oxo-1,4-dihydroquinoline-3-carboxylic acid 1b; Figure S14. ¹³C NMR spectrum (100 MHz, DMSO-d₆) of 7-(4-(5-amino-1-(p-tolyl)-1H-1,2,3-triazole-4-carbonyl)piperazin-1-yl)-1-ethyl-6-fluoro-4-oxo-1,4-dihydroquinoline-3-carboxylic acid 1b; Figure S15. LC/MS data for 7-(4-(5-amino-1-(p-tolyl)-1H-1,2,3-triazole-4-carbonyl)piperazin-1-yl)-1-ethyl-6-fluoro-4-oxo-1,4-dihydroquinoline-3-carboxylic acid 1b; Figure S16. IR spectrum of 7-(4-(5-amino-1-(p-tolyl)-1H-1,2,3-triazole-4-carbonyl)piperazin-1-yl)-1-ethyl-6-fluoro-4-oxo-1,4-dihydroquinoline-3-carboxylic acid 1b; Figure S17. UV/Vis spectrum of 7-(4-(5-amino-1-(p-tolyl)-1H-1,2,3-triazole-4-carbonyl)piperazin-1-yl)-1-ethyl-6-fluoro-4-oxo-1,4-dihydroquinoline-3-carboxylic acid 1b (0.08%DMSO/MeOH); Figure S18. ¹H NMR spectrum (400 MHz, DMSO-d₆) of 7-(4-(5-amino-1-(4-bromophenyl)-1H-1,2,3-triazole-4-carbonyl)piperazin-1-yl)-1-ethyl-6-fluoro-4-oxo-1,4-dihydroquinoline-3-carboxylic acid 1c; Figure S19. ¹³C NMR spectrum (100 MHz, DMSO-d₆) of 7-(4-(5-amino-1-(4-bromophenyl)-1H-1,2,3-triazole-4-carbonyl)piperazin-1-yl)-1-ethyl-6-fluoro-4-oxo-1,4-dihydroquinoline-3-carboxylic acid 1c; Figure S20. LC/MS data for 7-(4-(5-amino-1-(4-bromophenyl)-1H-1,2,3-triazole-4-carbonyl)piperazin-1-yl)-1-ethyl-6-fluoro-4-oxo-1,4-dihydroquinoline-3-carboxylic acid 1c; Figure S21. IR spectrum of 7-(4-(5-amino-1-(4-bromophenyl)-1H-1,2,3-triazole-4-carbonyl)piperazin-1-yl)-1-ethyl-6-fluoro-4-oxo-1,4-dihydroquinoline-3-carboxylic acid 1c; Figure S22. UV/Vis spectrum of 7-(4-(5-amino-1-(4-bromophenyl)-1H-1,2,3-triazole-4-carbonyl)piperazin-1-yl)-1-ethyl-6-fluoro-4-oxo-1,4-dihydroquinoline-3-carboxylic acid 1c (0.08%DMSO/MeOH); Figure S23. ¹H NMR spectrum (400 MHz, DMSO-d₆) of 7-(4-(5-amino-1-phenyl-1H-1,2,3-triazole-4-carbonyl)piperazin-1-yl)-1-cyclopropyl-6-fluoro-4-oxo-1,4-dihydroquinoline-3-carboxylic acid 2d; Figure S24. ¹³C NMR spectrum (100 MHz,

(4-bromophenyl)-1H-1,2,3-triazole-4-carbonyl)piperazin-1-yl)-1-cyclopropyl-6-fluoro-4-oxo-1,4-dihydroquinoline-3-carboxylic acid 2j; Figure S54. ¹³C NMR spectrum (100 MHz, DMSO-d₆) of 7-(4-(5-amino-1-(4-bromophenyl)-1H-1,2,3-triazole-4-carbonyl)piperazin-1-yl)-1-cyclopropyl-6-fluoro-4-oxo-1,4-dihydroquinoline-3-carboxylic acid 2j; Figure S55. LC/MS data for 7-(4-(5-amino-1-(4-bromophenyl)-1H-1,2,3-triazole-4-carbonyl)piperazin-1-yl)-1-cyclopropyl-6-fluoro-4-oxo-1,4-dihydroquinoline-3-carboxylic acid 2j; Figure S56. IR spectrum of 7-(4-(5-amino-1-(4-bromophenyl)-1H-1,2,3-triazole-4-carbonyl)piperazin-1-yl)-1-cyclopropyl-6-fluoro-4-oxo-1,4-dihydroquinoline-3-carboxylic acid 2j; Figure S57. UV/Vis spectrum of 7-(4-(5-amino-1-(4-bromophenyl)-1H-1,2,3-triazole-4-carbonyl)piperazin-1-yl)-1-cyclopropyl-6-fluoro-4-oxo-1,4-dihydroquinoline-3-carboxylic acid 2j (2%DMSO/MeOH); Figure S58. ¹H NMR spectrum (400 MHz, DMSO-d₆) of 7-(4-(5-amino-1-(5-fluoro-2-methylphenyl)-1H-1,2,3-triazole-4-carbonyl)piperazin-1-yl)-1-cyclopropyl-6-fluoro-4-oxo-1,4-dihydroquinoline-3-carboxylic acid 2k; Figure S59. ¹³C NMR spectrum (100 MHz, DMSO-d₆) of 7-(4-(5-amino-1-(5-fluoro-2-methylphenyl)-1H-1,2,3-triazole-4-carbonyl)piperazin-1-yl)-1-cyclopropyl-6-fluoro-4-oxo-1,4-dihydroquinoline-3-carboxylic acid 2k; Figure S60. LC/MS data for 7-(4-(5-amino-1-(5-fluoro-2-methylphenyl)-1H-1,2,3-triazole-4-carbonyl)piperazin-1-yl)-1-cyclopropyl-6-fluoro-4-oxo-1,4-dihydroquinoline-3-carboxylic acid 2k; Figure S61. IR spectrum of 7-(4-(5-amino-1-(5-fluoro-2-methylphenyl)-1H-1,2,3-triazole-4-carbonyl)piperazin-1-yl)-1-cyclopropyl-6-fluoro-4-oxo-1,4-dihydroquinoline-3-carboxylic acid 2k; Figure S62. UV/Vis spectrum of 7-(4-(5-amino-1-(5-fluoro-2-methylphenyl)-1H-1,2,3-triazole-4-carbonyl)piperazin-1-yl)-1-cyclopropyl-6-fluoro-4-oxo-1,4-dihydroquinoline-3-carboxylic acid 2k (0.08% DMSO/MeOH); Figure S63. ¹H NMR spectrum (400 MHz, DMSO-d₆) of 7-(4-(5-amino-1-(4-(trifluoromethyl)phenyl)-1H-1,2,3-triazole-4-carbonyl)piperazin-1-yl)-1-cyclopropyl-6-fluoro-4-oxo-1,4-dihydroquinoline-3-carboxylic acid 2l; Figure S64. ¹³C NMR spectrum (100 MHz, DMSO-d₆) of 7-(4-(5-amino-1-(4-(trifluoromethyl)phenyl)-1H-1,2,3-triazole-4-carbonyl)piperazin-1-yl)-1-cyclopropyl-6-fluoro-4-oxo-1,4-dihydroquinoline-3-carboxylic acid 2l; Figure S65. LC/MS data for 7-(4-(5-amino-1-(4-(trifluoromethyl)phenyl)-1H-1,2,3-triazole-4-carbonyl)piperazin-1-yl)-1-cyclopropyl-6-fluoro-4-oxo-1,4-dihydroquinoline-3-carboxylic acid 2l; Figure S66. IR spectrum of 7-(4-(5-amino-1-(4-(trifluoromethyl)phenyl)-1H-1,2,3-triazole-4-carbonyl)piperazin-1-yl)-1-cyclopropyl-6-fluoro-4-oxo-1,4-dihydroquinoline-3-carboxylic acid 2l; Figure S67. UV/Vis spectrum of 7-(4-(5-amino-1-(4-(trifluoromethyl)phenyl)-1H-1,2,3-triazole-4-carbonyl)piperazin-1-yl)-1-cyclopropyl-6-fluoro-4-oxo-1,4-dihydroquinoline-3-carboxylic acid 2l (0.08% DMSO/MeOH).

Author Contributions: Conceptualization, S.M.K. and V.G.; methodology, L.S.; software, L.P.; validation, L.P. and N.F.; formal analysis, L.S.; investigation, H.H., I.M., L.P., O.G.; resources, S.M.K.; data curation, I.M.; writing—original draft preparation, H.H., I.M.; writing—review and editing, S.M.K. and V.G.; visualization, L.P.; supervision, L.S., S.M.K. and V.G.; project administration, L.S.; funding acquisition, L.S. All authors have read and agreed to the published version of the manuscript.

Funding: Research was funded by the Ministry of Health of Ukraine from the state budget according to the topic ‘Molecular design and microbiological screening of innovative derivatives of fluoroquinolone antibiotics in order to combat resistant strains of microorganisms’ (state registration number: 0121U109239).

Institutional Review Board Statement: Not applicable.

Informed Consent Statement: Not applicable.

Conflicts of Interest: The authors declare no conflict of interest.

References

1. Beović, B.; Doušak, M.; Ferreira-Coimbra, J.; Nadrah, K.; Rubulotta, F.; Belliato, M.; Berger-Estilita, J.; Ayoade, F.; Rello, J.; Erdem, H. Antibiotic use in patients with COVID-19: A ‘snapshot’ Infectious Diseases International Research Initiative (ID-IRI) survey. *J. Antimicrob. Chemother.* **2020**, *75*, 3386–3390. [[CrossRef](#)] [[PubMed](#)]
2. Mohammed, H.H.; Abuo-Rahma, G.E.-D.A.; Abbas, S.; Abdelhafez, E.-S.M. Current Trends and Future Directions of Fluoroquinolones. *Curr. Med. Chem.* **2018**, *26*, 3132–3149. [[CrossRef](#)] [[PubMed](#)]
3. Lucia, P. Quinolones: Synthesis and Antibacterial Activity. *IntechOpen* **2012**, 255–272. [[CrossRef](#)]
4. Suaifan, G.A.; Mohammed, A.A. Fluoroquinolones structural and medicinal developments (2013–2018): Where are we now? *Bioorg. Med. Chem.* **2019**, *27*, 3005–3060. [[CrossRef](#)]
5. Zahoor, A.F.; Yousaf, M.; Siddique, R.; Ahmad, S.; Naqvi, S.A.R.; Rizvi, S.M.A. Synthetic strategies toward the synthesis of enoxacin-, levofloxacin-, and gatifloxacin-based compounds: A review. *Synth. Commun.* **2017**, *47*, 1021–1039. [[CrossRef](#)]

6. Zhang, G.-F.; Liu, X.; Zhang, S.; Pan, B.; Liu, M.-L. Ciprofloxacin derivatives and their antibacterial activities. *Eur. J. Med. Chem.* **2018**, *146*, 599–612. [[CrossRef](#)]
7. Lin, P.-Y.; Yeh, K.-S.; Su, C.-L.; Sheu, S.-Y.; Chen, T.; Ou, K.-L.; Lin, M.-H.; Lee, L.-W. Synthesis and Antibacterial Activities of Novel 4-Hydroxy-7-hydroxy- and 3-Carboxycoumarin Derivatives. *Molecules* **2012**, *17*, 10846–10863. [[CrossRef](#)]
8. Pisano, M.B.; Kumar, A.; Medda, R.; Gatto, G.; Pal, R.; Fais, A.; Era, B.; Cosentino, S.; Uriarte, E.; Santana, L.; et al. Antibacterial Activity and Molecular Docking Studies of a Selected Series of Hydroxy-3-arylcoumarins. *Molecules* **2019**, *24*, 2815. [[CrossRef](#)]
9. Cantón, R. Current microbiological aspects of community respiratory infection beyond COVID-19. *Rev. Esp. Quimioter.* **2021**, *34*, 81–92. [[CrossRef](#)]
10. Karampela, I.; Dalamaga, M. Could Respiratory Fluoroquinolones, Levofloxacin and Moxifloxacin, Prove to be Beneficial as an Adjunct Treatment in COVID-19? *Arch. Med. Res.* **2020**, *51*, 741–742. [[CrossRef](#)]
11. Marciniak, K.; Beberok, A.; Pećak, P.; Boryczka, S.; Wrześniok, D. Ciprofloxacin and moxifloxacin could interact with SARS-CoV-2 protease: Preliminary in silico analysis. *Pharmacol. Rep.* **2020**, *72*, 1553–1561. [[CrossRef](#)]
12. Scroggs, S.L.P.; Offerdahl, D.K.; Flather, D.P.; Morris, C.N.; Kendall, B.L.; Broeckel, R.M.; Beare, P.A.; Bloom, M.E. Fluoroquinolone Antibiotics Exhibit Low Antiviral Activity against SARS-CoV-2 and MERS-CoV. *Viruses* **2020**, *13*, 8. [[CrossRef](#)]
13. Oniga, S.; Palage, M.; Araniciu, C.; Marc, G.; Oniga, O.; Vlase, L.; Prisăcari, V.; Valica, V.; Curlat, S.; Uncu, L. Design, Synthesis, Molecular Docking, And Antibacterial Activity Evaluation of Some Novel Norfloxacin Analogues. *Farmacia* **2018**, *66*, 1048–1058. [[CrossRef](#)]
14. Marc, G.; Araniciu, C.; Oniga, S.; Vlase, L.; Pîrnău, A.; Nadăş, G.C.; Novac, C.; Matei, I.A.; Chifiriuc, M.C.; Mărutescu, L.; et al. Design, Synthesis and Biological Evaluation of New Piperazin-4-yl-(acetyl-thiazolidine-2,4-dione) Norfloxacin Analogues as Antimicrobial Agents. *Molecules* **2019**, *24*, 3959. [[CrossRef](#)]
15. Norouzbahari, M.; Salarinejad, S.; Güran, M.; Şanlıtürk, G.; Emamgholipour, Z.; Bijanzadeh, H.R.; Toolabi, M.; Foroumadi, A. Design, synthesis, molecular docking study, and antibacterial evaluation of some new fluoroquinolone analogues bearing a quinazolinone moiety. *DARU J. Pharm. Sci.* **2020**, *28*, 661–672. [[CrossRef](#)]
16. Mohammed, H.H.; Abbas, S.H.; Abdelhafez, E.S.M.; Berger, J.M.; Mitarai, S.; Arai, M.; Abu-Rahma, G.E.D.A. Synthesis, molecular docking, antimicrobial evaluation, and DNA cleavage assay of new thiadiazole/oxadiazole ciprofloxacin derivatives. *Monatshefte Chem.* **2019**, *150*, 1809–1824. [[CrossRef](#)]
17. Demirci, A.; Karayel, K.G.; Tatar, E.; Okullu, S.Ö.; Ünübol, N.; Taşlı, P.N.; Kocagöz, Z.T.; Şahin, F.; Küçükgüzel, I. Synthesis and evaluation of novel 1,3,4-thiadiazole fuoroquinolone hybrids as antibacterial, antituberculosis, and anticancer agents. *Turk. J. Chem.* **2018**, *42*, 839–858. [[CrossRef](#)]
18. Mokaber-Esfahani, M.; Eshghi, H.; Akbarzadeh, M.; Gholizadeh, M.; Mirzaie, Y.; Hakimi, M.; Lari, J. Synthesis and Antibacterial Evaluation of New Pyrimidyl N-Ciprofloxacin Derivatives. *ChemistrySelect* **2019**, *4*, 8930–8933. [[CrossRef](#)]
19. Yadav, P.; Hada, S.; Yadav, D.K.; Kumari, N. Synthesis and antibacterial activity of 1,3-dione derivatives of 1-cyclopropyl-7-[4-(2,6-dimethyl/ dimethoxy-pyrimidin-2-yl-diazenyl)-piperzin-1-yl]-6-fluoro-4-oxo-1,4-dihydroquinolone-3-carboxylic acid. *Indian J. Chem. Sect. B Org. Med. Chem.* **2018**, *57*, 1065–1069.
20. Li, Z.; Wang, Y.; Li, M.; Zhang, H.; Guo, H.; Ya, H.; Yin, J. Synthesis and properties of dithienylethene-functionalized switchable antibacterial agents. *Org. Biomol. Chem.* **2018**, *16*, 6988–6997. [[CrossRef](#)]
21. Mentese, M.; Demirbas, N.; Mermer, A.; Demirci, S.; Demirbas, A.; Ayaz, F.A. Novel Azole-Functionalited Fluoroquinolone Hybrids: Design, Conventional and Microwave Irradiated Synthesis, Evaluation as Antibacterial and Antioxidant Agents. *Lett. Drug Des. Discov.* **2018**, *15*, 46–64. [[CrossRef](#)]
22. Kharb, R.; Sharma, P.C.; Yar, M.S. Pharmacological significance of triazole scaffold. *J. Enzym. Inhib. Med. Chem.* **2010**, *26*, 1–21. [[CrossRef](#)] [[PubMed](#)]
23. Bylov, I.E.; Bilokin, Y.V.; Kovalenko, S.M. Specific Features of Reactions of 2-Aminobenzotrifluoride and Anthranilates with Ethyl Cyanoacetate—Expeditious Routes to 3-Substituted 4-Amino- and 4-Hydroxyquinolin-2(1 H)-Ones. *Heterocycl. Commun.* **1999**, *5*, 281–284. [[CrossRef](#)]
24. Silin, O.V.; Savchenko, T.I.; Kovalenko, S.M. Synthesis of 5H-Pyrazolo[4,3-c]quinolines. *Heterocycles* **2004**, *63*, 1883–1890. [[CrossRef](#)]
25. Savchenko, T.I.; Silin, O.V.; Kovalenko, S.M.; Musatov, V.I.; Nikitchenko, V.M.; Ivachtchenko, A.V. Alkylation of 3-Phenyl-1H-pyrazolo[4,3-c] quinoline: Theoretical Analysis of Regioselectivity. *Synth. Commun.* **2007**, *37*, 1321–1330. [[CrossRef](#)]
26. Mohapatra, R.K.; El-Ajaily, M.M.; Alassbaly, F.S.; Sarangi, A.K.; Das, D.; Maihub, A.A.; Ben-Gweirif, S.F.; Mahal, A.; Suleiman, M.; Perekhoda, L.; et al. DFT, anticancer, antioxidant and molecular docking investigations of some ternary Ni(II) complexes with 2-[(E)-[4-(dimethylamino)phenyl]methyleneamino]phenol. *Chem. Pap.* **2021**, *75*, 1005–1019. [[CrossRef](#)]
27. Mohapatra, R.K.; Perekhoda, L.; Azam, M.; Suleiman, M.; Sarangi, A.K.; Semenets, A.; Pintilie, L.; Al-Resayes, S.I. Computational investigations of three main drugs and their comparison with synthesized compounds as potent inhibitors of SARS-CoV-2 main protease (Mpro): DFT, QSAR, molecular docking, and in silico toxicity analysis. *J. King Saud Univ.-Sci.* **2021**, *33*, 101315. [[CrossRef](#)]
28. Bax, B.D.; Chan, P.F.; Eggleston, D.S.; Fosberry, A.; Gentry, D.R.; Gorrec, F.; Giordano, I.; Hann, M.M.; Hennessy, A.; Hibbs, M.; et al. Type IIA topoisomerase inhibition by a new class of antibacterial agents. *Nature* **2010**, *466*, 935–940. [[CrossRef](#)]
29. Blower, T.R.; Williamson, B.H.; Kerns, R.J.; Berger, J.M. Crystal structure and stability of gyrase-fluoroquinolone cleaved complexes from *Mycobacterium tuberculosis*. *Proc. Natl. Acad. Sci. USA* **2016**, *113*, 1706–1713. [[CrossRef](#)]

30. Laponogov, I.; Pan, X.-S.; Veselkov, D.A.; Cirz, R.T.; Wagman, A.; Moser, H.E.; Fisher, L.M.; Sanderson, M.R. Exploring the active site of the *Streptococcus pneumoniae* topoisomerase IV–DNA cleavage complex with novel 7,8-bridged fluoroquinolones. *Open Biol.* **2016**, *6*. [[CrossRef](#)]
31. Волянський, Ю.Л.; Гриценко, І.С.; Ширококов, В.П. Вивчення специфічної активності протимікробних лікарських засобів; ДФЦ МОЗ: Kiev, Ukraine, 2004; p. 38.
32. Визначення чутливості мікроорганізмів доантибактеріальних препаратів; Наказ МОЗ України №167 05.04.2007: Методичні вказівки; Ministry of Health of Ukraine: Kyiv, Ukraine, 2007.
33. Hryhoriv, H.; Mariutsa, I.; Kovalenko, S.M.; Sidorenko, L.; Perekhoda, L.; Filimonova, N.; Geyderikh, O.; Georgiyants, V. Structural modification of ciprofloxacin and norfloxacin for searching new antibiotics to combat drug-resistant bacteria. *Sci. Pharm. Sci.* **2021**, *5*, 4–11. [[CrossRef](#)]
34. Griбанov, P.S.; Topchiy, M.A.; Golenko, Y.D.; Lichtenstein, Y.I.; Eshtukov, A.V.; Terekhov, V.E.; Asachenko, A.F.; Nechaev, M.S. An unprecedentedly simple method of synthesis of aryl azides and 3-hydroxytriazenes. *Green Chem.* **2016**, *18*, 5984–5988. [[CrossRef](#)]
35. Agalave, S.; Maujan, S.R.; Pore, V.S. Click Chemistry: 1,2,3-Triazoles as Pharmacophores. *Chem.–Asian J.* **2011**, *6*, 2696–2718. [[CrossRef](#)]